International Journal of Refrigeration 158 (2024) 385–392

Contents lists available at ScienceDirect

International Journal of Refrigeration

journal homepage: www.elsevier.com/locate/ijrefrig

Performance analysis of a rotary desiccant wheel using polymer material with high water uptake and low regeneration temperature

Analyse des performances d'une roue déshydratante rotative utilisant un matériau polymère à forte absorption d'eau et à faible température de régénération

Yanan Xue, Qian Li, Ruzhu Wang, Tianshu Ge *

Institute of Refrigeration and Cryogenics, Shanghai Jiao Tong University, Shanghai, 200240, China

ARTICLE INFO

Keywords:
Polymer
Rotary desiccant wheel
Dehumidification
High adsorption capacity
Low regeneration temperature
Performance evaluation

Mots clés:
Polymère
Roue déshydratante rotative
Déshumidification
Capacité d'absorption élevée
Température de régénération basse
Évaluation des performances

ABSTRACT

Desiccant wheels have been widely used in humidity control, particularly under conditions with ultra-low dew point temperatures. However, traditional desiccants such as silica gel and zeolites are subject to relatively low adsorption capacity and high regeneration temperature. To address these challenges, a type of polymer material with high water uptake and low regeneration temperature is investigated in this paper. Firstly, the adsorption/desorption capacity of this polymer is thoroughly tested. Results reveal that its remarkable equilibrium adsorption capacity and desorption rate coefficients $k_{LDF,de}$ are 350% and 32–64% higher than that of silica gel, respectively. Moreover, its required regeneration temperature is just about 40–70 °C. The performance of the desiccant wheel using this polymer is simulated by a model validated by experiments tests. Parameter analysis demonstrates that the desiccant wheel is suitable for cool and humid conditions, reaching the maximum moisture removal (ΔY) and dehumidification coefficient of performance (DCOP) of 4.0 g kg^{-1} and 0.66, respectively. Furthermore, the corresponding relationship between other parameters and the optimal rotation speed is discussed in detail. The ω_{opt} is around 18 rph, enabling the attainment of the highest ΔY. Finally, the performance comparison with a traditional silica gel desiccant wheel is carried out. The results indicate that the polymer one performs 17–53.9% higher in terms of both ΔY and DCOP than the silica gel counterpart. And the most significant improvement is observed in low relative humidity conditions (45%RH), where ΔY and DCOP are 1.25–1.53 times that of the silica gel's, highlighting the advantageous utilization of the polymer material.

1. Introduction

Since the carbon peaking and carbon neutrality goals have been proposed, there has been a convergence of judgments from all sectors of society on the ways of energy transformation. As society evolves, the use of air conditioning systems increases, and the demand for energy-saving is more urgent (Li et al., 2022). However, traditional condensation dehumidification needs the air temperature to be cooled down below the dew point, which causes huge energy consumption. In order to solve this problem, solid dehumidification becomes a promising method, primarily due to its energy-efficient and environmentally friendly attributes (Abdullah et al., 2023). And desiccant wheel dehumidification attracts considerable attention because of its large moisture removal capacities and continuous regeneration mechanisms (Chen et al., 2022), which offers an excellent solution to practical humidity control.

For the desiccant wheel, the desiccant material is the key factor to affecting its dehumidification performance. Hence, extensive research has been conducted to investigate and understand the properties of desiccant materials, which aims to enhance their overall performance. In which, silica gels (Kenz and Novak, 2001) and zeolites (Wei Benjamin Teo et al., 2017) have been commonly chosen for desiccant wheels due to their good adaptability (Minqi et al., 2021), stable characteristics and low cost (Vivekh et al., 2018; Zheng et al., 2014). However, these pure conventional desiccants are subject to low adsorption capacity and high regeneration temperature.

Impregnating hygroscopic salts in conventional desiccant materials was proved to be an effective method to enhance the water sorption capacity. The composite of $CaCl_2$ and silica gel achieved a sorption capacity of 0.95 g g^{-1} at 90%RH (Alsaman et al., 2022). The zeolite

* Corresponding author.
E-mail address: baby_wo@sjtu.edu.cn (T. Ge).

https://doi.org/10.1016/j.ijrefrig.2023.12.003
Received 11 August 2023; Received in revised form 1 November 2023; Accepted 3 December 2023
Available online 4 December 2023

Nomenclature

a	half height of the flow passage (m)
b	half wide of the flow passage (m)
c_p	constant pressure specific heat (kJ (kg K)$^{-1}$)
f	specific mass (kg m^{-1})
H_v	evaporation latent heat of water (kJ kg^{-1})
h	specific enthalpy (kJ kg^{-1})
k	kinetic constant (s^{-1})
L	desiccant wheel thickness (m)
m	mass (kg)
Nu	Nusselt number
p	pressure (Pa)
q_{st}	sorption heat (kJ kg^{-1})
r	radius of desiccant (m)
RH	relative humidity
Sh	Sherwood number
T	temperature (K)
t	time (s)
V	flow rate (m s^{-1})
W	extent of adsorption (kg^{-1})
Y	air moisture content (kg^{-1})
Z	direction of axial (m)

Greek symbols

θ	dimensionless water uptake of desiccant layer
λ	thermal conductivity of dry air (W (m K)$^{-1}$)
ω	rotation speed (rph)

Subscripts

0	initial state
∞	final state
a	air
d	desiccant
l	liquid water
m	matrix
p	process air
r	regeneration air
v	water vapor
w	gas-solid partition surface
amb	ambient
ad	adsorption
de	desorption
in	inlet
out	outlet
opt	optimal value

impregnated by $CaCl_2$, LiBr, $MgSO_4$, $LiNO_3$, and $Ca(NO)_3$ salts, and the results indicated an increase in water adsorption from 0.28 to 0.6 g g^{-1} for all composites at RH > 60% (Alsaman et al., 2022). Besides, binary salt composites also improve dehumidification, adding LiBr to the LiCl composites of silica gel intensifies the sorption capacity up to 5.5% (Entezari et al., 2018). And by impregnating with binary salts ($LiCl+CaCl_2$), the composite of zeolite 13X and SAPO-34 indicated 5.3 times and 4 times water uptake performance than their porous matrixes (Elwadood et al., 2023; Zhao et al., 2020). However, the corrosion, deliquescence, and spill-over phenomenon caused by the usage of hygroscopic materials (Bilal and al., 2022) limits the application of salt composite desiccant.

In addition to the composites impregnated with hygroscopic salt, there is ongoing exploration of advanced materials. For example, metal-organic frameworks (MOFs) received much attention due to their exceptional physicochemical features (Liu and al., 2021). Though the high water adsorption capacity under a wide range of working pressure and medium desorption temperature make them promising adsorbents (Mohseni et al., 2022), high costs and the inability to scale up production have hindered their widespread commercial utilization.

Based on this, polymers show a promising investigation value in recent years, mainly because of their high water uptake capacity and low regeneration temperature (Zheng et al., 2014). It has been reported that the polymer desiccant achieved a 2-3 times high sorption capacity compared to silica gel and represented a more excellent performance under high relative humidity conditions (Lee and Lee, 2012). Meanwhile, the regeneration temperature is relatively low compared to conventional desiccant materials (White et al., 2011). Due to the superior performance of polymers, many researchers are attracted to studying the application of polymers in dehumidification. Cao et al. (2014) conducted the parameter analysis of the polymer desiccant wheel with the regeneration temperature of 60 °C, they found that lower inlet air temperature and higher humidity ratio are in favor of better dehumidification performance, and the moisture removal of the thin polymer desiccant wheels (50 and 70 mm) shown 1.2 and 0.7 times higher than the 150 mm wheel. Kang and Lee (2017) observed the dehumidification effectiveness of the polymer desiccant wheel is 1.11–2.24 times that of other silica gel's, while also displaying a smaller sensible temperature increase. Additionally, Zhou et al. (2018) proposed a novel tube-shell, internally water-cooled desiccant wheel with polymer desiccant channels, which indicated an improved dehumidification performance of around 48% and an energy efficiency ratio of 9.3.

Nevertheless, an all-around understanding of the relationship between the relative parameters and the heat/mass transfer of polymer based desiccant wheel has not yet been accomplished. In this paper, firstly, the polymer adsorbent is prepared and investigated, which indicates the high water uptake characteristic from the equilibrium adsorption, and reveals the reason why the polymer is suitable for low-regeneration temperature from the kinetics of sorption. Then, the performance of the polymer desiccant wheel is simulated, and the accuracy of the mathematical model was verified through experiments. The parametric analysis of the polymer desiccant wheel is thoroughly discussed, with a specific focus on analyzing the influence of the optimal rotation speed. Finally, the application suitability of the polymer desiccant wheel is also discussed through the comparison with the silica gel desiccant wheel, which can give suggestions to maximize the advantages of the application of the polymer desiccant wheel.

2. Description of polymer adsorbent

One kind of polymer composed of polyacrylonitrile is adopted. The morphology of the polymer adsorbent can be found in the supporting information Fig. S1. The equilibrium adsorption curve of this polymer is tested using ASAP 2020PLUS micromeritics and is compared with that of a widely used silica gel (Wu, 2019), as shown in Fig. 1. It can be seen that with the same relative pressure, the polymer shows higher equilibrium adsorption capacity. Notably, in comparison the curve of the polymer with a steep slope at the low relative pressure (below 0.3) and high relative pressure (above 0.7). This phenomenon indicates that the polymer is more sensitive to changes in regeneration temperature and exhibits better equilibrium adsorption capacity under high relative pressures.

The kinetics of water vapor adsorption/desorption is vital for practical applications of desiccant materials (Mittal et al., 2020). And the details of the adsorption/desorption kinetics experiments are shown in supporting materials Table S1 and Fig. S2. The adsorption kinetics experiment is conducted at 20 °C and 80%RH and the desorption kinetics experiment is then carried out at different regeneration

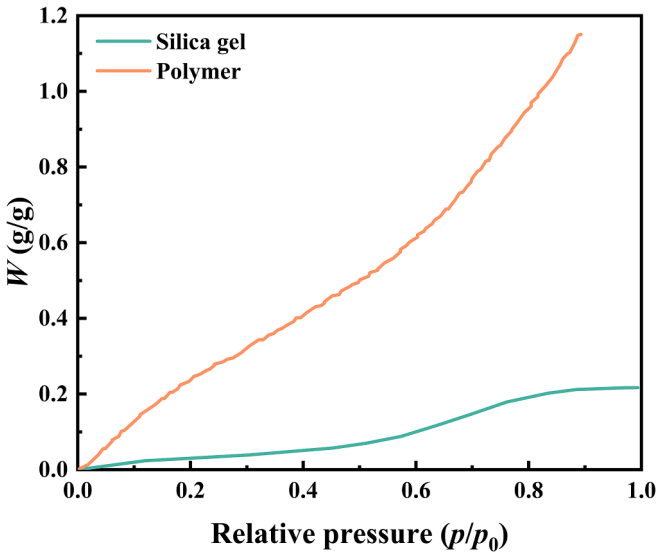

Fig. 1. Equilibrium adsorption curves of the polymer and silica gel.

temperatures of 40 °C, 50 °C, 60 °C, and 70 °C, respectively. As a comparison, the kinetic analysis of the silica gel has also been studied.

To evaluate the kinetics results, the linear driven force (LDF) model was commonly used. The mass change of the desiccant layer for the adsorption process can be expressed by Liu et al. (2022):

$$m = m_\infty - (m_\infty - m_0)\exp(-k_{LDF,ad}t) \quad (1)$$

The mass change of the desiccant layer for the desorption process can be described by Liu et al. (2022):

$$m = m_\infty + (m_0 - m_\infty)\exp(-k_{LDF,de}t) \quad (2)$$

where the m means the instant water uptake, the subscript 0 and ∞ present the initial and equilibrium state, and adsorption rate coefficient $k_{LDF,ad}$ and desorption rate coefficient $k_{LDF,de}$ refer to the kinetic constant of the adsorption process and the desorption process.

The regression from the LDF approximation of the adsorption process is shown in Fig. 2(a). The equilibrium water uptake of the polymer is 4.5 times of the silica gel, and the adsorption rate of the polymer is 2.6 times that of the silica gel, because of the advantage of the equilibrium adsorption capacity. But $k_{LDF,ad}$ of the polymer is lower than that of the silica gel. Fig. 2(b) and Fig. S3(a) depict the regression from LDF approximation of polymer and silica gel under various regeneration temperatures respectively. Significantly, under low regeneration temperatures (40–70 °C), the $k_{LDF,de}$ of the polymer are all higher than the silica gel (Fig. S3(b)).

The comparison results of $k_{LDF,ad}$ and $k_{LDF,de}$ can be explained the change of the adsorbent thickness. The thickness of the polymer is 126.8 μm at complete desorption and 166.8 μm at equilibrium adsorption (Fig. S4). Thus, the thickness of the polymer increases during adsorption and gets thinner during desorption, which affects the mass transfer resistance.

There is a remarkable improvement in the desorption rate and $k_{LDF,ad}$ of the polymer over the silica gel. Thus, due to the dominant desorption performance, the regeneration time can be greatly shortened. For a polymer desiccant wheel, the angle of the regeneration side can be decreased to improve the performance of the dehumidification. With the faster desorption rate, the reasonable rotation speed of the polymer desiccant wheel is higher than that of the silica gel.

3. Mathematical model and validation

An established gas-side resistance model (Ge and al., 2008) is used to predict the performance of such polymer desiccant wheel. Both the assumptions and governing equations are the same as in reference (Zhang et al., 2003), the main differences are the auxiliary conditions as shown in the following. Table 1 displays the geometrical parameters and physical parameters used in the simulation and experiment.

The relative humidity on the adsorbent surface (RH_w) can be calculated by the equilibrium water uptake (W) of adsorbent. And the equilibrium adsorption equation is fitted by the equilibrium adsorption curves of the polymer.

$$RH_w = 0.0086 + 0.6396W - 0.2174W^2 + 7.7601W^3 - 18.6552W^4 + 16.3083W^5 - 4.9321W^6 \quad (3)$$

A polymer desiccant wheel is produced, as Fig. S5 illustrates. An experimental system as shown in Fig. S6 is established to validate the accuracy of the model, and the details of the experiment can be found in supporting information. The experiment is carried out with typical operating parameters (Table 2). The predicted results in terms of temperature and humidity ratio of outlet air from the process side agree well with the experimental data, with discrepancies of most conditions less

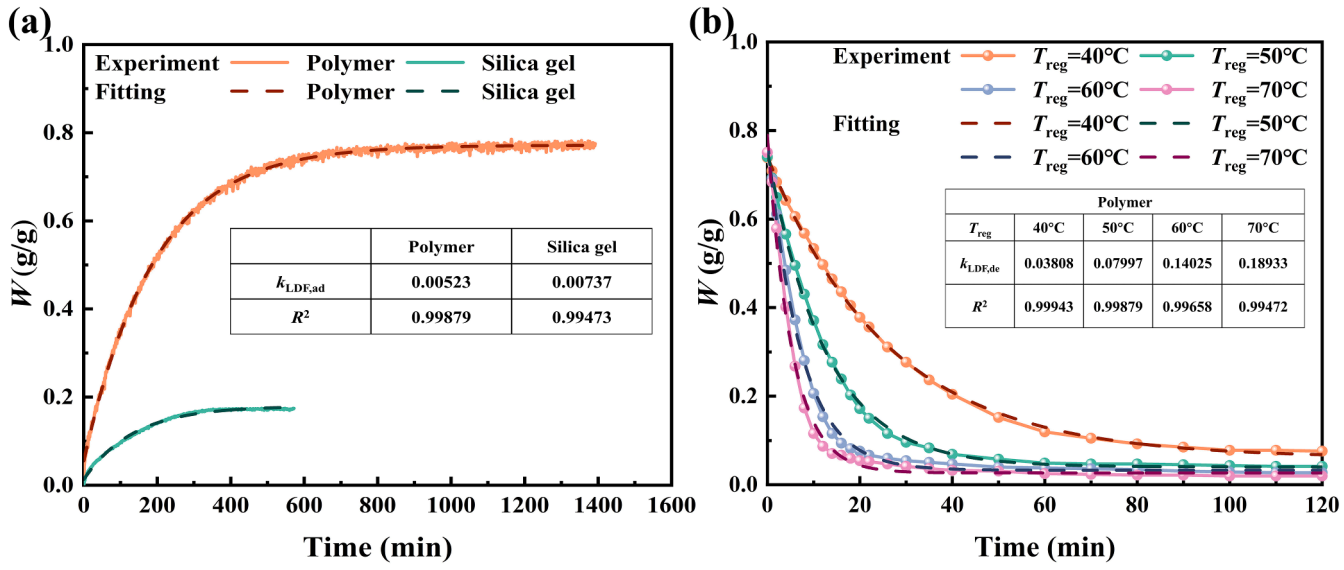

	Polymer	Silica gel
$k_{LDF,ad}$	0.00523	0.00737
R^2	0.99879	0.99473

Polymer				
T_{reg}	40°C	50°C	60°C	70°C
$k_{LDF,de}$	0.03808	0.07997	0.14025	0.18933
R^2	0.99943	0.99879	0.99658	0.99472

Fig. 2. Kinetic analysis. (a)Adsorption kinetics comparison of polymer and silica gel under 20 °C and relative humidity of 80%. (b) Desorption kinetics of polymer.

Table 1
Some parameters and the corresponding values involved in numerical simulation and experiment.

The geometrical size of desiccant wheel			
Half height of the flow passage, a(m)	0.00085	Half wide of the flow passage, b(m)	0.0017
Nu_z	2.12	Sh_z	2.12
Thickness of desiccant wheel, L(m)	0.2	Radius of desiccant wheel, r (m)	0.125
Specific desiccant mass, f_d(kg m^{-1})	0.00016	Specific matrix mass, f_m(kg m^{-1})	0.0002
The thermodynamic properties of desiccant			
Specific heat of the polymer, C_{pd}(J (kg K)$^{-1}$)	1510	Specific heat of matrix material, C_{pm}(J (kg K)$^{-1}$)	1321
The corresponding properties of moist air			
Thermal conductivity of dry air, λ(W (m K)$^{-1}$)	0.0230	Specific heat of dry air, C_{pa}(J (kg K)$^{-1}$)	1009
Specific heat of water vapor, C_{pv}(J (kg K)$^{-1}$)	2028.1	Specific heat of water, C_{pl}(J (kg K)$^{-1}$)	4179
Evaporation latent heat of water, H_v(kJ kg^{-1})	2358		

Table 2
Operating parameters of experiments.

Parameters	Baseline values	Parametric variations
Rotation speed, ω	15 rph	3–24 rph
Angel of regeneration air side	90°	–
Temperature of the ambient air, T_{amb}	20 °C	10–40 °C
Humidity ratio of ambient air, Y_{amb}	8.73 g kg^{-1}	4.56–21.44 g kg^{-1}
Flow rate of process air, V_p	2.5 m s^{-1}	1.5–3.5 m s^{-1}
Flow rate of regeneration air, V_r	2.5 m s^{-1}	1.5–3.5 m s^{-1}
Regeneration temperature, T_{reg}	70 °C	40–70 °C

than 10% (Fig. 3). However, at low humidity ratio conditions (e.g., 4.56 g kg^{-1}), the relative error appears to be significant owing to small values of the experimented/simulated outlet humidity ratio of the process air. Nevertheless, the deviation is still within 20%. Thus, the accuracy of the mathematical model has been verified.

4. Simulation results and discussion

4.1. Performance indices

Moisture removal ΔY is chosen to evaluate the dehumidification capacity of desiccant wheel.

$$\Delta Y = Y_{p,in} - Y_{p,out} \left[\text{g kg}^{-1}\right] \tag{4}$$

Another index, the dehumidification coefficient of performance (DCOP) (Adi Saputra et al., 2020; Liu et al., 2022; Ma et al., 2023), indicates the efficiency of the energy utilization, which measures how much of the energy input to the regeneration side is efficiently gained by the latent heat in the process side. A higher DCOP is preferred which means less heat is wasted to heat the desiccant wheel.

$$DCOP = \frac{m_p H_v \Delta Y}{m_r \left(h_{r,in} - h_{amb}\right)} \tag{5}$$

4.2. Effects of operation parameters

The analysis of operating parameters and the applicability in different environmental working conditions are conducted. The operating parameters are listed in Table 3.

4.2.1. Effect of rotation speed

ΔY and DCOP under various rotation speeds ω of 3–27 rph, and regeneration temperature T_{reg} ranging from 40 °C to 70 °C are illustrated in Fig. 4. As ω increases, ΔY first increases obviously and then decreases slightly. This is mainly because when ω is below 15 rph, the equilibrium time of the adsorbent is much shorter than the rotation cycle, which means that a part of adsorbent in process side is at equilibrium state and this region is useless. As ω increases, the useful region of the process side continues to increase, resulting in the increase of ΔY. When ω is above 15 rph, the entire process section has adsorption capacity. Thus, a further increase of ω displays little effect on ΔY. Meanwhile, the increase in ω will increase the heat loss between the regeneration side and the process side, resulting in the reduction of the temperature difference between these two sides, which is not conducive to dehumidification.

Table 3
Operating parameters of simulations.

Parameters	Baseline values	Parametric variations
Rotation speed, ω	15 rph	3–27 rph
Angel of regeneration air side	90°	–
Temperature of the ambient air, T_{amb}	25 °C	10–40 °C
Humidity ratio of ambient air, Y_{amb}	11.93 g kg^{-1}	4.75–21.44 g kg^{-1}
Process air flow rate, V_p	2.5 m s^{-1}	1.5–3.5 m s^{-1}
Regeneration air flow rate, V_r	2.5 m s^{-1}	1.5–3.5 m s^{-1}
Regeneration temperature, T_{reg}	60 °C	40–70 °C

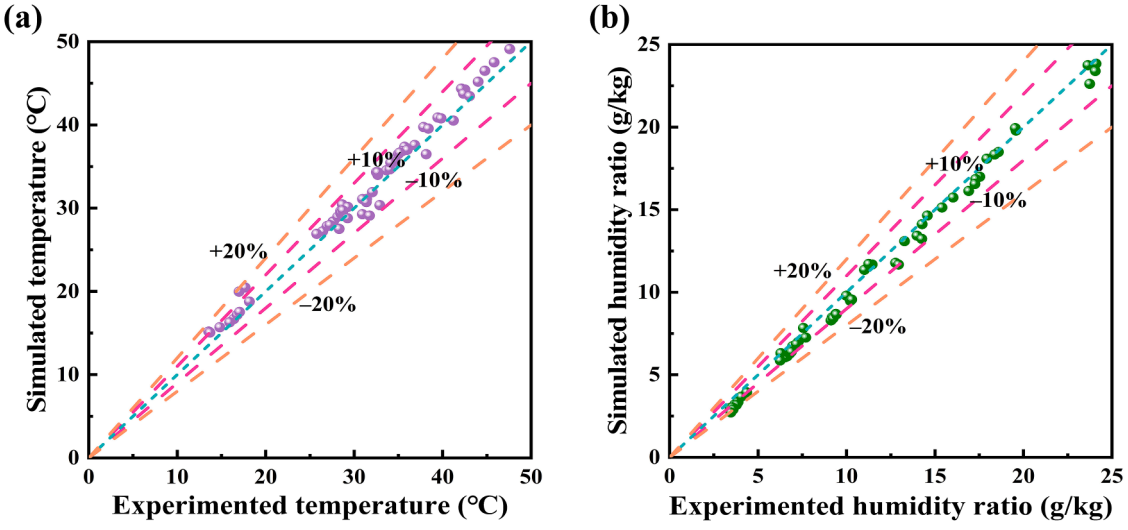

Fig. 3. The error of the temperature(a) and the humidity ratio(b) between the simulated and experimental results.

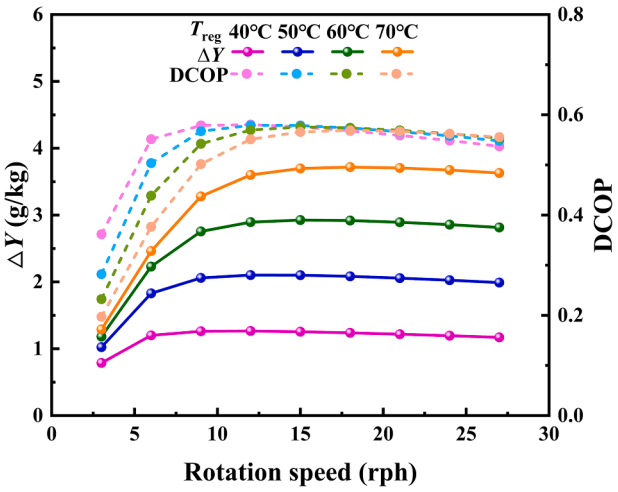

Fig. 4. Effect of the rotation speed on moisture removal and DCOP.

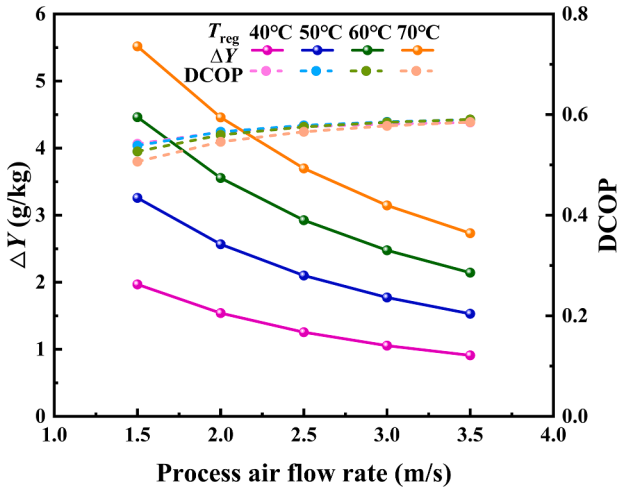

Fig. 5. Effect of the process air flow rate on moisture removal and DCOP.

This explains the reason why at high-speed range (15–27 rph), the values of ΔY are basically the same but with a slight decrease. DCOP changes in the same way as ΔY because the regeneration energy input keeps the same. Considering the dehumidification capacity and energy utilization efficiency at the same time, the recommended ω of this polymer desiccant is 15 rph. In this case, when T_{reg} increase from 40 °C to 70 °C, ΔY is 1.25 g kg^{-1}, 2.10 g kg^{-1}, 2.93 g kg^{-1}, and 3.70 g kg^{-1}, respectively, and meanwhile, DCOP is 0.576, 0.579, 0.576, and 0.566, respectively.

4.2.2. *Effect of regeneration temperature*

Fig. 4 illustrates that a greater ΔY is gained when T_{reg} rises from 40 °C to 70 °C. This is because a higher moisture concentration gradient between desiccant and regeneration air is created and both the desorption rate as well as desorption capacity are improved. The maximum ΔY values at T_{reg} = 40 °C, 50, 60, and 70 °C are 1.26 g kg^{-1}, 2.10 g kg^{-1}, 2.92 g kg^{-1}, and 3.72 g kg^{-1}, respectively. And the stable growth rate of ΔY indicates that the adsorption potential of this desiccant material is less limited at low T_{reg}, which is mainly due to the characteristic of the equilibrium adsorption curve of the polymer being convex at low relative humidity (0–30%). As for DCOP, at low ω (below 15 rph), it decreases as the T_{reg} increases, which is because the energy input into the rotor is more significant than the ΔY increment obtained from the process side. However, when the ω is higher than 15 rph, the difference of DCOP under various T_{reg} is smaller. Because, at this point, the changing trend of ΔY and the energy input the rotor are consistent. It is also worth noting that the increase of T_{reg} will also cause a higher outlet temperature on the process side, which means a greater sensible heat load needs to be disposed of by the subsequent refrigeration equipment. Thus, in practical applications, the T_{reg} should be carefully selected according to specific demand, system performance, and available heat source.

4.2.3. *Effect of the process air flow rate*

Fig. 5 shows the influence of process air flow rate V_p. When the V_p varies from 1.5 m s^{-1} to 3.5 m s^{-1}, the lower V_p is conducive to ΔY, and the reason is explained as followed. The total moisture removal capacity increases with the increase of V_p (Fig. S7), which reflects that with the variation of V_p the desiccant does not reach the equilibrium adsorption. So it can be inferred that the adsorption rate increases with the increasing V_p, and the adsorption capacity also increases since the desiccant is not in equilibrium. However, the increase of the mass of process air is more significant than the increase of the adsorption capacity. And the growth rate of the total moisture removal slows down at high V_p, which is mainly due to the higher the V_p, the greater the cooling rate of the process air. Thus, the lower the outlet temperature of the process air, the larger the heat loss occurs on the regeneration side, which is not good for further dehumidification. The changing trend of DCOP is the same as total moisture removal. When V_p changes from 1.5 m s^{-1} to 3.5 m s^{-1}, DCOP varies from 0.54 to 0.58, 0.54 to 0.59,0.53 to 0.59, and 0.51 to 0.58, which corresponds to the T_{reg} of 40 °C, 50 °C, 60 °C, and 70 °C, respectively. In this way, to pursue the optimal utilization of the energy, setting the V_p around 2.0 m s^{-1}–2.5 m s^{-1} is reasonable.

4.2.4. *Effect of the regeneration air flow rate*

The impacts of the regeneration air flow rate V_r are plotted in Fig. 6. Taking the T_{reg} of 70 °C as an example, ΔY changes from 2.34 g kg^{-1} to 4.35 g kg^{-1} when the V_r increases from 1.5 m s^{-1} to 3.5 m s^{-1}. ΔY increases as V_r increases, while its growth rate slows down. On the one hand, a higher V_r facilitates the regeneration heat energy input, and more energy can be converted into the latent heat in adsorbed moisture during the subsequent dehumidification process. On the other hand, when V_r further increases, the heat loss from the regeneration side to the process side increases, which limited the ΔY to a degree and thereby decelerates the increase rate. In terms of DCOP, a higher V_r means that more energy input is required to heat ambient air to the desired regeneration temperature, causing a decrease of DCOP. At T_{reg} = 40 °C, 50 °C, 60 °C, 70 °C, DCOP decreases from 0.57 to 0.54, 0.58 to 0.52, 0.59 to 0.50, and 0.60 to 0.47, respectively, when V_r increases from 1.5 m s^{-1} to 3.5 m s^{-1}. From the analysis above, a practical V_r around 2.5 m s^{-1} is

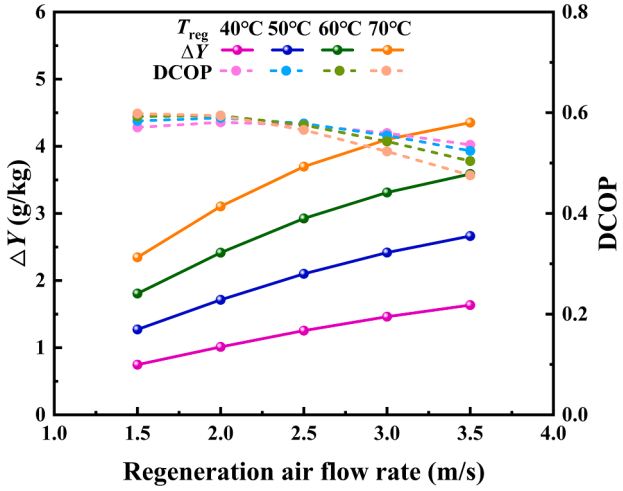

Fig. 6. Effect of the regeneration air flow rate on moisture removal and DCOP.

recommended to pursue a high ΔY and DCOP simultaneously.

4.2.5. Effect of the external environment: ambient temperature

As the T_{reg} increases from 40 °C to 70 °C, the dehumidification performance under the same humidity ratio (21 g kg^{-1}) but different ambient temperatures T_{amb} (28 °C, 34 °C, and 40 °C) are simulated, and results are illustrated in Fig. 7. The lower the T_{amb}, the greater the ΔY. When the T_{reg} varies from 40 °C to 70 °C with the T_{amb} of 28 °C, ΔY is 1.17 g kg^{-1}, 2.15 g kg^{-1}, 3.11 g kg^{-1}, and 4.04 g kg^{-1}, respectively. Compared with the T_{amb} of 40 °C, in which case T_{reg} = 40 °C can not take effect when the T_{reg} increases from 50 °C to 70 °C, ΔY (T_{amb} of 28 °C) increases by 131.5%, 70.2%, and 51.1%, respectively. This is mainly because when the humidity ratio is constant, the lower the T_{amb}, the greater the relative humidity of the inlet air stream, which means a more significant partial pressure of water vapor in the air stream and a stronger adsorption capacity of the desiccant. However, the lower the T_{amb} the heat loss increases which is not conducive to dehumidification. Under all investigated T_{amb}, DCOP decreases slightly as T_{reg} increases. This is mainly because the change of the energy input is more significant than the increase of ΔY. Except for the low-regeneration condition (T_{reg} = 40 °C), DCOP decreases with the increase of the T_{amb}, which can be explained that though the energy input is less, the ΔY also gets lower and the change of ΔY accounts for the main factor. The figure can be explained why the DCOP of 34 °C is a little higher than that of the 28 °C, when the T_{reg} is 40 °C the adsorption capacity of the desiccant at each T_{amb} is weak, and the energy input to the system becomes the main factor determining DCOP. The cool external condition is preferable for the polymer desiccant wheel. However, in low regeneration temperature conditions, lowering the T_{amb} does not work well. Thus, there is a reasonable T_{amb} at different ambient humidity ratios. In practical application, it is necessary to consider comprehensively and not mindlessly reducing the inlet temperature of the process side.

4.2.6. Effect of the external environment: ambient relative humidity

Fixing T_{amb} to 25 °C and varying RH_{amb} from 40 % to 80 %, ΔY and DCOP are displayed in Fig. 8. ΔY increases with the increase of the RH_{amb}, and at high T_{reg} the advantage of ΔY at high RH_{amb} becomes more apparent, which is owing to a more complete regeneration process. Under each T_{reg} (40 °C-70 °C), with the RH_{amb} increasing from 40 % to 80 %, ΔY is from 1.05 g kg^{-1} to 1.36 g kg^{-1}, 1.77 g kg^{-1} to 2.28 g kg^{-1}, 2.47 g kg^{-1} to 3.18 g kg^{-1}, and 3.09 g kg^{-1} to 4.05 g kg^{-1}, respectively. Because a higher RH_{amb} means the gradient of partial water vapor pressure between the air stream and the desiccant is greater, which is more conducive to adsorption. Meanwhile, the T_{amb} is the same, so the heat loss of the desiccant wheel is approximately the same even at high

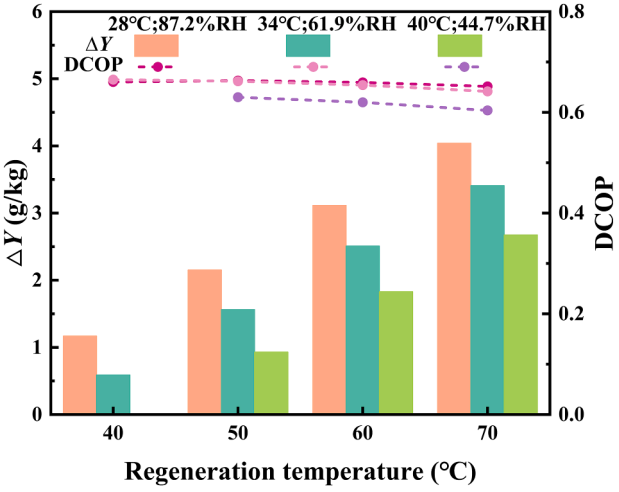

Fig. 7. Effect of the ambient temperature on moisture removal and DCOP.

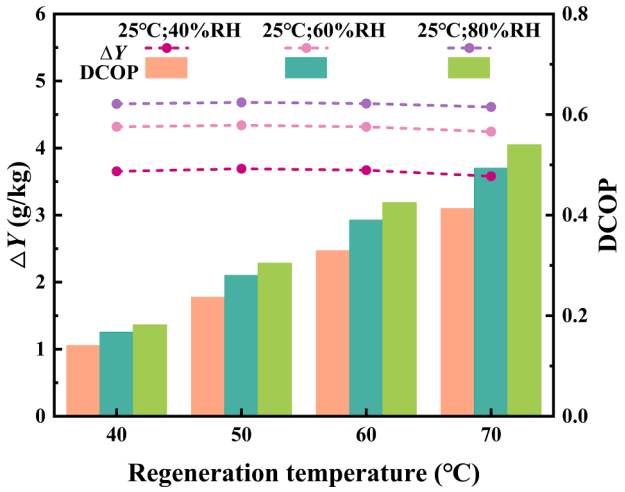

Fig. 8. Effect of the ambient humidity ratio on moisture removal and DCOP.

RH_{amb}, and further dehumidification capacity is not limited. DCOP increases with the increase of RH_{amb}, this is mainly due to the increase of ΔY is more significant than the increase of energy input. At a certain RH_{amb}, DCOP is basically the same at various T_{reg}, which is mainly because the changing trend of the energy input and ΔY are essentially the same. Based on the simulation results above, the polymer desiccant wheel is suitable for operating under humid conditions. Thus, installing precooling equipment before the inlet of the process air to increase the RH_{amb} is beneficial for achieving higher dehumidification capacity.

4.3. Investigation of the optimal rotation speed

ω is crucial to ΔY of the desiccant wheel, and there always exists an optimal rotation speed ω_{opt} at each specific working condition. So it is essential to regulate ω reasonably for the maximum ΔY. The influence of the T_{reg} on the ω_{opt} can be figured out in Fig. 4. ω_{opt} increases gradually when T_{reg} improves from 40 °C to 70 °C. ω_{opt} is 12 rph when the T_{reg} is 40 °C and 50 °C, and it increases to 15 rph at 60 °C, and 18 rph at 70 °C. Because the desorption rate increases with the increase of T_{reg}, the regeneration side can rotate to the process side in time for the following adsorption leading to a higher ω_{opt}. And the effect of the other parameters (V_p, V_r, T_{amb}, RH_{amb}) is discussed as follows.

As illustrated in Fig. 9, V_p has a relatively small impact on ω_{opt}. ω_{opt} keeps constant at 18 rph when V_p increases from 1.5 m s^{-1} to 3.5 m s^{-1}. As V_p increases, the adsorption rate increases leading to a higher ω_{opt}. On the other hand, the average temperature of the process air decreases which indicates a greater adsorption capacity leading to a lower ω_{opt}. Based on these two points, the ω_{opt} does not change with the variation of V_p. On the contrary, V_r has a notable effect on ω_{opt}, which increases from 9 rph to 27 rph, when V_r varies from 1.5 m s^{-1} to 3.5 m s^{-1}. With the increase of V_r, the desorption rate increases obviously and the average temperature of the regeneration air also increases which relates to a better desorption capacity, both of them inducing a higher ω_{opt}. Thus, a higher ω_{opt} is needed to make the regeneration side move into the process side in time.

As for the influence of T_{amb} and RH_{amb}, the ω_{opt} increases from 12 rph to 21 rph, when T_{amb} varies from 28 °C to 40 °C. The potential of the adsorption capacity is poorer at a higher T_{amb}. In this way, the ω_{opt} needs to increase to avoid the desiccant being saturated. The ω_{opt} decreases from 21 rph to 15 rph, when RH_{amb} increases from 40% to 80%. Though a higher RH_{amb} improves the adsorption rate, from the regeneration side, a high RH_{amb} is not conducive to desorption. So a lower ω_{opt} is needed to ensure a more sufficient regeneration process.

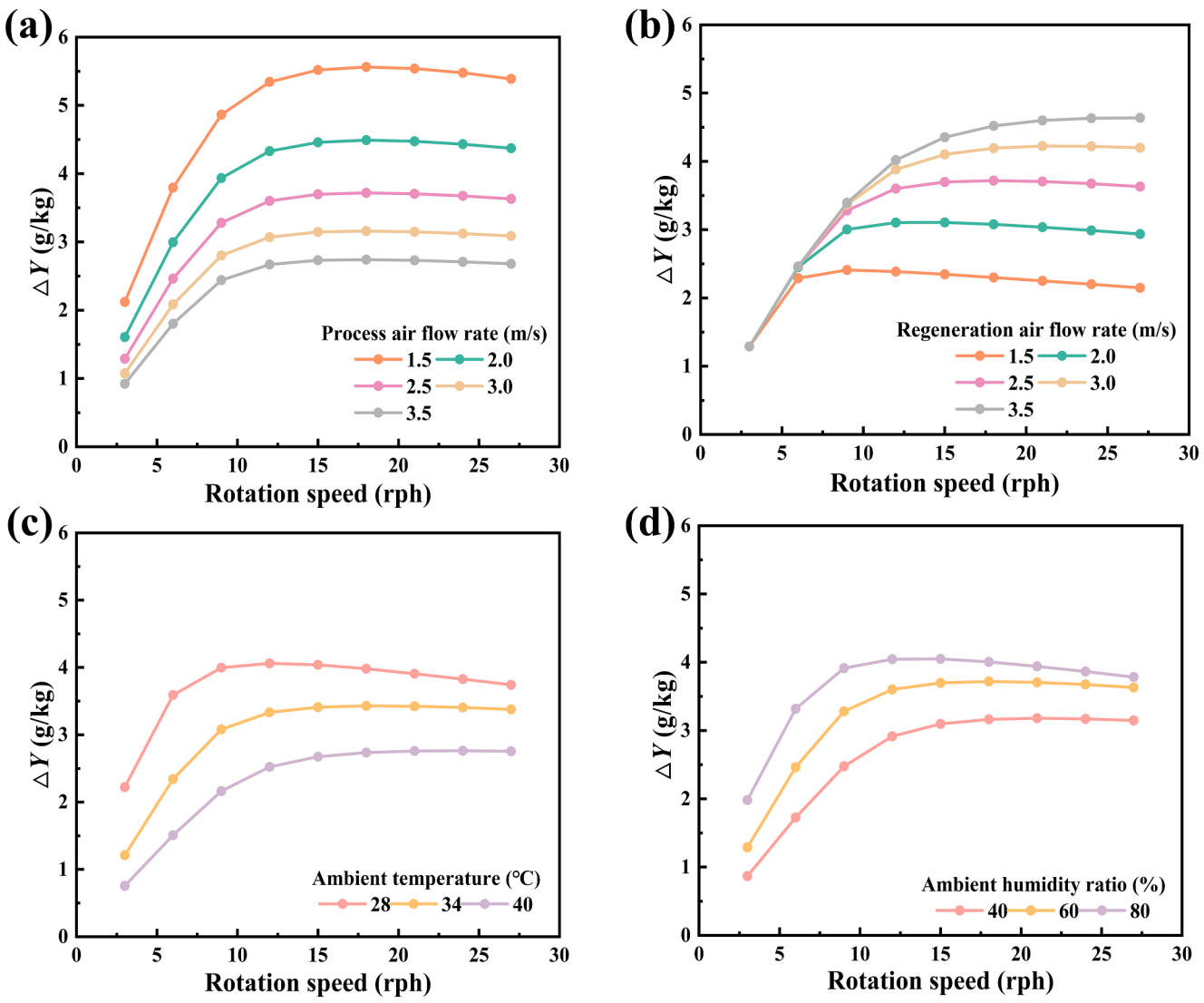

Fig. 9. Moisture removal with the variation of rotation speed (a) process air flow rate, (b) regeneration air flow rate, (c) ambient temperature and (d) ambient humidity ratio.

4.4. Performance comparison with traditional silica gel desiccant wheel

The performance of the polymer desiccant wheel is compared with conventional silica gel desiccant under varied T_{reg} (results of T_{reg} = 60 °C in Fig. 10 and T_{reg} = 40 °C, 50 °C, 70 °C in Fig. S8). The adsorption isotherm of silica gel and other parameters are derived from the former literature (Wu, 2019; Zhang et al., 2003). Five edge operational conditions for a wide range of environment are selected as listed in Table 4.

Compared with the silica gel desiccant wheel, the polymer one shows a greater ΔY and DCOP under all the operational conditions. And the changing trend of DCOP is consistent with ΔY. Specifically, the polymer's ΔY values are 31.2–53.9%, 17.1–32.4%, 23.1–41.6%, 24.9–41.6%, and 18.5–34.8% higher than silica gel's, corresponding to conditions (I–V).

From the comparative analysis, the polymer desiccant wheel demonstrates a greater deep dehumidification capacity at low relative humidity conditions (I and IV), which indicates that the polymer desiccant wheel is more suitable for the realization of low dew point conditions. And the low-temperature conditions (15 °C) are more favorable by the polymer desiccant wheel because of the higher ΔY. In this way, the upstream of polymer rotor compounding with precooling equipment, like an evaporator, which has more advantages and can obtain a better

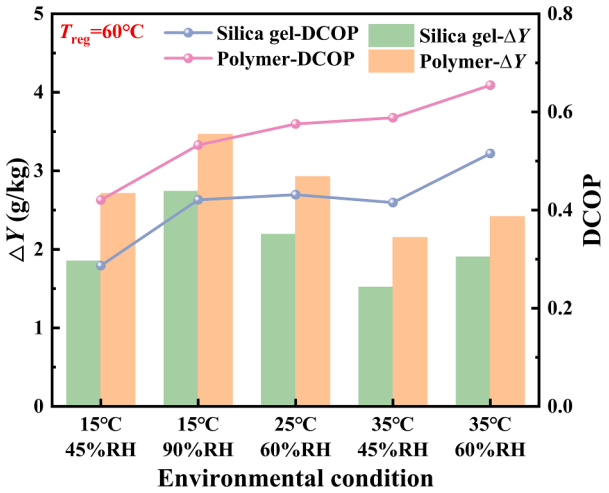

Fig. 10. Comparison of the silica gel and polymer in terms of the moisture removal ΔY and DCOP, T_{reg} is 60 °C.

Table 4
Five edge operational conditions for a wide range of environment.

Number	Typical working condition	Temperature and relative humidity
I	low temperature and low humidity	15 °C;45%RH
II	low temperature and high humidity	15 °C;90%RH
III	moderate condition	25 °C;60%RH
IV	high temperature and low humidity	35 °C;45%RH
V	high temperature and high humidity	35 °C;60%RH

dehumidification potential.

5. Conclusion

To evaluate the performance of the polymer desiccant wheel, the adsorption as well as desorption characteristics of the desiccant material are tested and the parameter analysis of the polymer desiccant wheel is simulated. The main results are summarized below:

(1) The equilibrium adsorption capacity of the polymer at 90%RH is 1.15g g^{-1}, which is five times that of silica gel. The adsorption/desorption kinetic experiments reflect that the adsorption rate of the polymer is 2.6 times that of silica gel, and the $k_{LDF,de}$ of the polymer is 1.32–1.64 times that of silica gel with the T_{reg} of 40–70 °C, which demonstrates the polymer's suitability for low-temperature regeneration.
(2) ΔY increases with the decrease of V_p and T_{amb} and the increase of V_r, T_{reg}, and RH_{amb}. DCOP increases with the decrease of V_r and T_{amb} and the increase of V_p and RH_{amb}. As the ω increases, ΔY and DCOP first increase and then decrease slightly. When Treg increases from 40 °C to 70 °C, DCOP decreases at low ω (below 15 rph) and increases at high ω (above 15 rph).
(3) ω_{opt} exists to achieve the best ΔY. Under the basic condition, 15 rph is recommended as a reasonable rotation speed. And the value of ω_{opt} increases with the increase of T_{reg}, V_r, and T_{amb}, but decreases with the increase of RH_{amb}, and keeps constant with the variation of V_p.
(4) Compared with the traditional silica gel desiccant wheel, a cool and dry condition can better highlight the advantages of the polymer. Therefore, the polymer desiccant wheel is more suitable for deep dehumidification. And precooling equipment is recommended to be used for the maximum dehumidification potential.

In summary, such a polymer desiccant wheel becomes a promising method to achieve low dew point dehumidification, which has a bright application prospect in the lithium battery industry, textile industry, biomedical, etc. Based on the advantage of low-temperature regeneration, it also can be integrated with heat pump, renewable energy, and industrial waste heat, which is expected to provide a hopeful solution for energy saving and sustainable development.

Declaration of Competing Interest

The authors declare that they have no known competing financial interests or personal relationships that could have appeared to influence the work reported in this paper.

Supplementary materials

Supplementary material associated with this article can be found, in the online version, at doi:10.1016/j.ijrefrig.2023.12.003.

References

Abdullah, S., et al., 2023. Technological development of evaporative cooling systems and its integration with air dehumidification processes: a review. Energy Build. 283, 112805.
Adi Saputra, D., et al., 2020. Experimental investigation of desiccant wheel dehumidification control method for changes in regeneration heat input. Energy 205, 118109.
Alsaman, A., et al., 2022a. Characterization and cost analysis of a modified silica gel-based adsorption desalination application. J. Clean. Prod. 379, 134614.
Alsaman, A.S., et al., 2022b. Composite adsorbent materials for desalination and cooling applications: a state of the art. Int. J. Energy Res. 46 (8), 10345–10371.
Bilal, M., et al., 2022. Adsorption-based atmospheric water harvesting: a review of adsorbents and systems. Int. Commun. Heat Mass Transf. 133, 105961.
Cao, T., et al., 2014. Experimental investigations on thin polymer desiccant wheel performance. Int. J. Refrig. 44, 1–11.
Chen, L., Chu, Y., Deng, W., 2022. Experimental investigation of dedicated desiccant wheel outdoor air cooling systems for nearly zero energy buildings. Int. J. Refrig. 134, 265–277.
Elwadood, S., et al., 2023. Hybrid salt-enriched micro-sorbents for atmospheric water sorption. J. Water Process Eng. 52, 103560.
Entezari, A., Ge, T.S., Wang, R.Z., 2018. Water adsorption on the coated aluminum sheets by composite materials (LiCl + LiBr)/silica gel. Energy 160, 64–71.
Ge, T.S., et al., 2008. A review of the mathematical models for predicting rotary desiccant wheel. Renew. Sustain. Energy Rev. 12 (6), 1485–1528.
Kang, H., Lee, D.-Y., 2017. Experimental investigation and introduction of a similarity parameter for characterizing the heat and mass transfer in polymer desiccant wheels. Energy 120, 705–717.
Kenz, Z., Novak, Z., 2001. Adsorption of water vapor on silica, alumina, and their mixed oxide aerogels. J. Chem. Eng. Data: ACS J. Data 46 (4), 858–860.
Lee, J., Lee, D.-Y., 2012. Sorption characteristics of a novel polymeric desiccant. Int. J. Refrig. 35 (7), 1940–1949.
Li, W., Yin, Y., Wang, Y., 2022. Performance evaluation of a heat pump-driven liquid desiccant dehumidification system integrated with fresh air supply. Energy Build. 275, 112473.
Liu, C., et al., 2021. MOF-on-MOF hybrids: synthesis and applications. Coord. Chem. Rev. 432, 213743.
Liu, L., et al., 2022a. Experimental and theoretical study on water vapor isothermal adsorption-desorption characteristics of desiccant coated adsorber. Int. J. Heat Mass Transf. 187, 122529.
Liu, Z., et al., 2022b. Experimental evaluation of the dehumidification performance of a metal organic framework desiccant wheel. Int. J. Refrig. 133, 157–164.
Ma, Z., Liu, X., Zhang, T., 2023. Experimental investigation and effectiveness analysis of a desiccant wheel dehumidification system with low air humidity. Appl. Therm. Eng. 226, 120279.
Minqi, S., et al., 2021. Experimental study on the performance of an improved dehumidification system integrated with precooling and recirculated regenerative rotary desiccant wheel. Appl. Therm. Eng. 199, 117608.
Mittal, H., Al Alili, A.R., Alhassan, S.M., 2020. Adsorption isotherm and kinetics of water vapors on novel superporous hydrogel composites. Microporous Mesoporous Mater. 299, 110106.
Mohseni, M., et al., 2022. Metal-organic frameworks (MOF) based heat transfer: a comprehensive review. Chem. Eng. J. 449, 137700.
Vivekh, P., et al., 2018. Recent developments in solid desiccant coated heat exchangers – a review. Appl. Energy 229, 778–803.
Wei Benjamin Teo, H., Chakraborty, A., Fan, W., 2017. Improved adsorption characteristics data for AQSOA types zeolites and water systems under static and dynamic conditions. Microporous Mesoporous Mater. 242, 109–117.
White, S.D., et al., 2011. Characterization of desiccant wheels with alternative materials at low regeneration temperatures. Int. J. Refrig. 34 (8), 1786–1791.
Wu, X.N., 2019. Theoretical and Experimental Investigation On Preferred Substrate Embedded With Silica Gel and Coupled Adsorptiom. Shanghai Jiao Tong University, p. 47.
Zhang, X.J., Dai, Y.J., Wang, R.Z., 2003. A simulation study of heat and mass transfer in a honeycombed rotary desiccant dehumidifier. Appl. Therm. Eng. 23 (8), 989–1003.
Zhao, H., et al., 2020. Water sorption on composite material "zeolite 13X modified by LiCl and CaCl2. Microporous Mesoporous Mater. 299, 110109.
Zheng, X., Ge, T.S., Wang, R.Z., 2014. Recent progress on desiccant materials for solid desiccant cooling systems. Energy 74, 280–294.
Zhou, X., Goldsworthy, M., Sproul, A., 2018. Performance investigation of an internally cooled desiccant wheel. Appl. Energy 224, 382–397.